



*On Frequency Offset Estimation Using the iNET
Preamble in Frequency Selective Fading
Channels*

March 2014

**Tom Young
SET Executing Agent
412 TENG/ENI
(661) 277-1071
Email: tommy.young.1@us.af.mil**

DISTRIBUTION STATEMENT A. Approved for public release: distribution unlimited.

**Test Resource Management Center (TRMC)
Test & Evaluation/ Science & Technology (T&E/S&T)
Spectrum Efficient Technology (SET)**

On Frequency Offset Estimation Using the iNET Preamble in Frequency Selective Fading Channels

Michael Rice
Brigham Young University
Provo, UT 84602
Email: mdr@byu.edu

Erik Perrins
The University of Kansas
Lawrence, KS 66045
Email: esp@ieee.org

Abstract—This paper develops five data-aided frequency offset estimators for SOQPSK-TG equipped with the iNET preamble and operating in ISI channels. Four of the five estimators examined here are generalizations of frequency estimators developed for the AWGN channel. Simulations, performed over channel impulse responses measured in multipath scenarios encountered in aeronautical telemetry, show the modified L&R estimator is the best in terms of tracking range and achievable mean-squared error. The ESP estimator is a close second and offers a computational complexity advantage in that it only requires the computation of one correlation value as opposed to the five correlation values required by the L&R estimator.

I. INTRODUCTION

The recent introduction of the iNET (for integrated Network Enhanced Telemetry) standard [1] provides a mode for packetized telemetry downlinks. Each packet comprises three bit fields: a preamble, an attached sync marker (ASM), and data bits (an LDPC codeword). The availability of a preamble introduces the possibility of data-aided synchronization in aeronautical telemetry. Compensating for carrier frequency and phase offsets and timing delay offsets is required for optimum coherent detection. Multipath interference, in the form of frequency selective fading, complicates the synchronization problem. Propagation through frequency selective fading introduces inter-symbol interference (ISI) into the received signal, and ISI can wreak havoc on estimators designed for the additive white Gaussian noise (AWGN) channel. For frequency offset estimation, the usual approach is to use a preamble with some periodic structure. With proper preprocessing, frequency offset estimators designed for the AWGN channel may then be applied, such as the maximum likelihood estimator formulated by Rife and Boorstyn [2], and the reduced-complexity estimators described by Kay [3], Fitz [4], Luise & Reggiannini [5], and Mengali & Morelli [6]. A nice example in the open literature is from Harris and Dick [7].

In this paper, we examine the problem of estimating the frequency offset in an ISI channel using SOQPSK-TG with the iNET preamble. We exploit the periodic structure of the

iNET preamble to develop a low-complexity frequency offset estimator with good performance.

II. PRELIMINARIES

The bit sequence for iNET is organized as outlined in the top portion of Figure 1. The preamble sequence is the iNET standard is CD98_{hex} repeated eight times [1, p. 48]. This bit pattern, derived from the analysis presented in [8], included the repetition to enable fast acquisition. Here, the periodic component associated with the repetition is leveraged to enable low-complexity frequency offset estimation.

The transmitted signal, $s(t)$, is SOQPSK-TG whose input bit stream is summarized in the top portion of Figure 1. SOQPSK-TG is a partial response CPM waveform with a constrained ternary alphabet. The details are spelled out in [9], [10]. The signal propagates through a frequency selective channel and experiences a frequency offset and the addition of additive white Gaussian noise. We assume the received signal is filtered, down-converted to complex baseband, and sampled (not necessarily in that order) using standard techniques. The resulting sequence of received samples is

$$r(n) = \left[\sum_{k=-N_1}^{N_2} h(k)s(n-k) \right] e^{j\omega_0 n} + w(n) \quad (1)$$

where $h(n)$ is the impulse response of the unknown channel impulse response with support on $-N_1 \leq n \leq N_2$, ω_0 rads/sample is the frequency offset to be estimated, and $w(n)$ is a proper [11] complex-valued zero-mean Gaussian random process with auto-covariance function

$$\frac{1}{2} \mathbb{E} \{ w(n)w^*(n-k) \} = \sigma_w^2 \delta(k). \quad (2)$$

Because SOQPSK-TG is a nonlinear modulation, the estimator cannot operate on the symbols in the same way it does for linear modulation. Consequently, the estimator must operate on the samples of SOQPSK-TG. Let i be the index in $r(n)$ corresponding to the beginning of the preamble sequence and let L_p be the number of samples in the preamble sequence. The situation is illustrated in Figure 1. Because each sample depends on the unknown channel impulse response $h(n)$, the standard approaches cannot be applied directly. However, an estimator that leverages the periodic properties of the iNET preamble can be applied.

This work was supported by the Test Resource Management Center (TRMC) Test and Evaluation Science and Technology (T&E/S&T) Program through a grant from the Army PEO STRI Contracting Office under contract W900KK-13-C-0026.

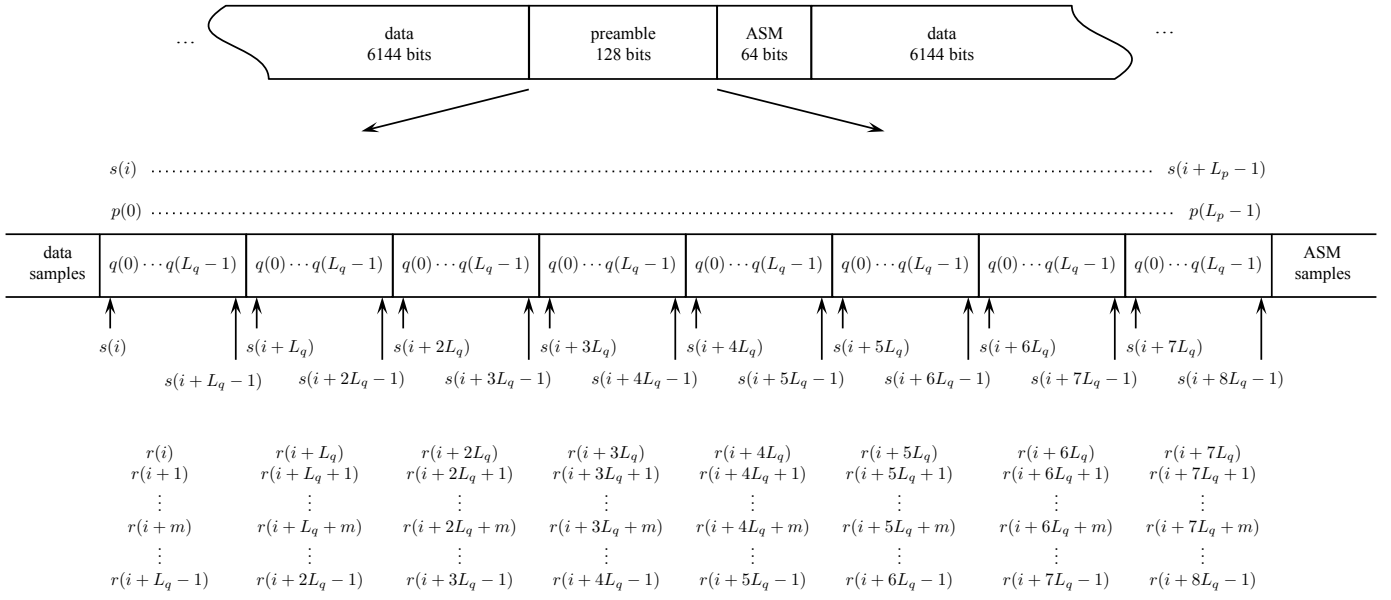


Fig. 1. A graphical illustration of the iNET data packet structure: (top) the data, preamble, and ASM fields; (bottom) the relationship between the indexes of the received samples $r(n)$, the signal samples $s(n)$, the preamble samples $p(n)$ and the short sequences $q(n)$ that constitute the preamble sequence.

Because the iNet preamble comprises 8 repetitions of a 16 bit sequence, the resulting SOQPSK-TG modulated carrier is also periodic over the time interval corresponding to the occurrence of the preamble. Furthermore the sampled SOQPSK-TG signal is periodic over the interval corresponding to the preamble sequence. The situation is illustrated in Figure 1. Here, $s(n)$ are the samples of the complex baseband SOQPSK-TG signal and $p(n')$ for $n' = 0, 1, \dots, L_p - 1$ are the samples of the complex baseband SOQPSK-TG signal corresponding to the preamble bits. If the preamble sequence starts at index i , then $s(i) = p(0)$, $s(i + 1) = p(1)$ and so on to $s(i + L_p - 1) = p(L_p - 1)$. Now let $q(n)$ be the samples of the complex baseband SOQPSK-TG signal corresponding to the 16-bit sequence that is repeated to form the preamble, and let the length of $q(n)$ be L_q . (At an equivalent sample rate of 2 samples/bit, $L_p = 256$ and $L_q = 32$.)

For $n = i, i + 1, \dots, i + L_p - 1$, we write $r(n) = r(i + b)$ for $b = 0, 1, \dots, L_p - 1$ and express it as follows:

$$r(i + b) = \left[\sum_{k=-N_1}^{N_2} h(k)s(i + b - k) \right] e^{j\omega_0(i+b)} + w(i + b) \quad (3)$$

$$= \left[\sum_{k=-N_1}^{N_2} h(k)p(b - k) \right] e^{j\omega_0(i+b)} + w(i + b). \quad (4)$$

To incorporate the periodic nature of $p(n)$ into the equation, we write

$$b = \ell L_q + m, \quad \ell = 0, 1, \dots, 7, \quad m = 0, 1, \dots, L_q - 1. \quad (5)$$

Here we see that ℓ indexes the block and m indexes the sample

within the block. Substituting gives

$$\begin{aligned} r(i + \ell L_q + m) &= \\ & \left[\sum_{k=-N_1}^{N_2} h(k)p(\ell L_q + m - k) \right] e^{j\omega_0(i+\ell L_q+m)} + w(i + \ell L_q + m) \\ &= \underbrace{\left[\sum_{k=-N_1}^{N_2} h(k)q(m - k) \right]}_{\alpha(m)} e^{j\omega_0(i+\ell L_q+m)} + w(i + \ell L_q + m). \quad (6) \end{aligned}$$

The relationship (6) is important. It shows that the contribution of the channel to $r(i + \ell L_q + m)$ depends only on m , the position inside the $q(\cdot)$ block. Consequently, the only difference (other than the additive noise) between the sample at position m in adjacent blocks is the phase rotation due to the frequency offset.¹ This feature is captured by the correlation function.

Assuming $N_1 < L_q$ and $N_2 < L_q$, we are interested in the correlation function involving the middle six blocks:

$$R(\delta) = \frac{1}{6L_q - \delta} \sum_{n=i+L_q+\delta}^{i+7L_q-1} r(n)r^*(n - \delta) \quad (7)$$

Because the samples $r(n)$ are periodic with period L_q , we are interested in evaluating this function at integer multiples

¹This is only true for middle six blocks (i.e., $\ell = 1, \dots, 6$) because the convolution sum in the first block ($\ell = 0$) includes samples from the data field immediately preceding the first block whereas the last block $\ell = 7$ includes samples from the ASM field immediately following the last block. Eliminating the first and last blocks is sufficient as long as $N_1 < L_q$ and $N_2 < L_q$. If either of these conditions are not true, then (6) is true for fewer blocks.

of L_q . For $\delta = dL_q$ ($1 \leq d \leq 5$) the correlation is (see the Appendix)

$$R(dL_q) = \frac{\alpha^2}{L_q} e^{jdL_q\omega_0} + v \quad (8)$$

where α^2 is given by

$$\alpha^2 = \sum_{m=0}^{L_q-1} |\alpha(m)|^2 \quad (9)$$

and v is approximately a complex-valued Gaussian random variable with zero mean and variance (39).

An obvious estimator is the delay-and-multiply (D&M) estimator (cf Eq. (4.5.1) of [12])

$$\hat{\omega}_0 = \frac{1}{L_q} \arg \left\{ R(L_q) \right\}. \quad (10)$$

This estimator is simple and exploits the noise averaging that occurs over the $5L_q$ consecutive samples of $r(n)$. But this estimator only uses $R(L_q)$. It would seem there might be performance advantages to incorporating the information in $R(2L_q)$, $R(3L_q)$, $R(4L_q)$, and $R(5L_q)$. To see how this might be done, we first look to how this same concept is applied in the AWGN case. Next we modify the developments to create frequency estimators for present case.

III. DATA-AIDED FREQUENCY ESTIMATORS FOR AWGN

The standard model for data-aided frequency estimators in the additive white Gaussian noise environment is the sinusoid in noise.

$$x(n) = e^{j\omega_0 n} + w(n) \quad (11)$$

for $n = 0, \dots, N-1$. The sinusoid in noise model is usually obtained from the sampled matched filter outputs at the receiver by multiplying each matched filter output by the conjugate of the corresponding pilot symbol. The maximum likelihood (ML) estimator is [2]

$$\hat{\omega}_0 = \underset{\omega_0}{\operatorname{argmax}} \left\{ \left| \sum_{n=0}^{N-1} x(n) e^{-j\omega_0 n} \right|^2 \right\}. \quad (12)$$

In words, the ML estimate is the one that maximizes the periodogram of the sequence $x(n)$. Because there is no closed form solution, this approach involves a search. For computational complexity reasons, a suboptimal solution that does not require a search is desirable. The most common data-aided estimators operate on the $x(n)$ or the autocorrelation function of the $x(n)$.

Fitz Estimator: The Fitz estimator is [4]

$$\hat{\omega}_0 = \frac{2}{M(M+1)} \sum_{m=1}^M m \left(\arg \left\{ \hat{R}_x(m) \right\} \right) \quad (13)$$

where $\hat{R}_x(m)$ is the unnormalized autocorrelation function

$$\hat{R}_x(m) = \sum_{n=m}^{N-1} x(n)x^*(n-m). \quad (14)$$

L&R Estimator: The Luise and Reggiannini (L&R) estimator is [5]

$$\hat{\omega}_0 = \frac{2}{M+1} \arg \left\{ \sum_{m=1}^M R_x(m) \right\} \quad (15)$$

where $R_x(m)$ is the normalized autocorrelation function

$$R_x(m) = \frac{1}{N-m} \sum_{n=m}^{N-1} x(n)x^*(n-m). \quad (16)$$

M&M Estimator: The Mengali and Morelli (M&M) estimator is [6]

$$\hat{\omega}_0 = \frac{\mathbf{1}^\top \mathbf{C}^{-1} \boldsymbol{\phi}}{\mathbf{1}^\top \mathbf{C}^{-1} \mathbf{1}}. \quad (17)$$

Here, $\mathbf{1}$ is the $M \times 1$ all-ones vector and

$$\boldsymbol{\phi} = [\phi(1) \quad \phi(2) \quad \dots \quad \phi(M)]^\top \quad (18)$$

where

$$\phi(m) = \arg \{ R_x(m) \} - \arg \{ R_x(m-1) \} \quad (19)$$

is the phase difference between successive autocorrelation functions (16). (The phase differences are used to overcome the phase wrapping problem with $\arg\{\cdot\}$.) \mathbf{C} is the $M \times M$ covariance matrix of the noise samples associated with the autocorrelation phase differences.

Kay Estimator: The Kay estimator is [3]

$$\hat{\omega}_0 = \frac{\mathbf{1}^\top \mathbf{C}^{-1} \boldsymbol{\Delta}}{\mathbf{1}^\top \mathbf{C}^{-1} \mathbf{1}} \quad (20)$$

where $\mathbf{1}$ is the $(N-1) \times 1$ all-ones vector, $\boldsymbol{\Delta}$ is the $(N-1) \times 1$ vector

$$\boldsymbol{\Delta} = [\Delta(1) \quad \Delta(2) \quad \dots \quad \Delta(N-1)]^\top \quad (21)$$

where

$$\Delta(n) = \arg \{ x(n)x^*(n-1) \} \quad (22)$$

is the phase difference between adjacent $x(n)$, and \mathbf{C} is the $(N-1) \times (N-1)$ covariance vector of the noise samples accompanying the phase differences.

IV. EXTENSIONS TO INET PREAMBLE-BASED FREQUENCY ESTIMATORS FOR ISI CHANNELS

In the previous section, we saw that the Fitz, L&R, and M&M estimators used information in the autocorrelation function (both unnormalized and normalized) of the received data samples. The modification of the Fitz, L&R, and M&M estimators more complicated than simply substituting $R(dL_q)$ [see (7)] for $R_x(m)$. This is because the sample spacing between the $R(dL_q)$ is L_q samples instead of one sample for $R_x(m)$. This not only impacts the noise correlations but also modifies the approximations applied in the intermediate steps in the derivations. Because space limitations do not permit a detailed accounting of all these steps, only the final results are listed here.

Modified Fitz Estimator: The modified Fitz estimator is

$$\hat{\omega}_0 = \frac{1}{55L_q} \sum_{m=1}^5 m \arg \left\{ \hat{R}(mL_q) \right\} \quad (23)$$

where $\hat{R}(mL_q) = ((6-m)L_q)R(mL_q)$ where $R(mL_q)$ is given by (7) for $m = 1, 2, 3, 4, 5$.

Modified L&R Estimator: The modified L&R estimator is

$$\hat{\omega}_0 = \frac{1}{3L_q} \arg \left\{ \sum_{m=1}^5 R(mL_q) \right\} \quad (24)$$

$R(mL_q)$ is given by (7) for $m = 1, 2, 3, 4, 5$.

Modified M&M Estimator: The modified M&M estimator is

$$\hat{\omega}_0 = \frac{1}{35L_q} \left[5\phi(L_q) + 8\phi(2L_q) + 9\phi(3L_q) + 8\phi(4L_q) + 5\phi(5L_q) \right] \quad (25)$$

where

$$\phi(mL_q) = \arg \left\{ R(mL_q) \right\} - \arg \left\{ R((m-1)L_q) \right\} \quad (26)$$

for $m = 1, 2, 3, 4, 5$.

Modified Kay Estimator: The modified Kay estimator is

$$\hat{\omega}_0 = \frac{1}{35L_q} \sum_{m=0}^{L_q-1} \frac{|\alpha(m)|^2}{\alpha^2} \left(5\Delta_{m,2} + 8\Delta_{m,3} + 9\Delta_{m,4} + 8\Delta_{m,5} + 5\Delta_{m,6} \right) \quad (27)$$

where

$$\Delta_{m,\ell} = \arg \left\{ r(i + \ell L_q + m)r^*(i + (\ell-1)L_q + m) \right\}.$$

The challenge with this form of the estimator is that the $\alpha(m)$ are unknown. The $\alpha(m)$ are used to weight each block of phase differences (and this weighting is in proportion to the relative channel output power). A suboptimal approach is to set the weights to be equal:

$$\frac{|\alpha(m)|^2}{\alpha^2} \approx \frac{1}{L_q}. \quad (28)$$

The result is

$$\hat{\omega}_0 = \frac{1}{35L_q^2} \sum_{m=0}^{L_q-1} \left(5\Delta_{m,2} + 8\Delta_{m,3} + 9\Delta_{m,4} + 8\Delta_{m,5} + 5\Delta_{m,6} \right). \quad (29)$$

V. SIMULATION RESULTS

The estimators were applied to three representative channel impulse responses capture during channel sounding experiments at Edwards AFB, California [13]. These channels are illustrated in Figure 2. See the figure caption for more details. In these simulations, the iNET preamble described in Section II was used with SOQPSK-TG operating at 10.3125 Mibts/s, the “over-the-air rate” corresponding to a payload bit

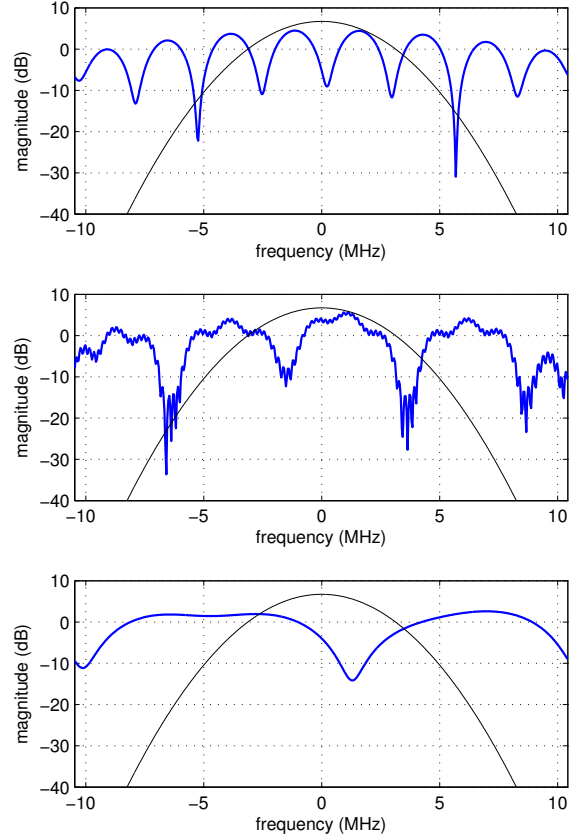


Fig. 2. The example channels from channel sounding experiments at Edwards AFB: (top) a length-9 channel from the flight line; (middle) a length-19 channel from take-off; (bottom) a length-5 channel from low-elevation angle “up and away” flight. In each plot, the thick line is the channel frequency response and the thin line is the power spectral density of SOQPSK-TG operating at 10.3125 Mbits/s.

rate of 10 Mbits/s. The channel and SOQPSK-TG preamble signal operated at a sample rate equivalent to 2 samples/bit.

As the performance measures, we use the means and variances of the Perrins (ESP), Fitz, L&R, M&M, and Kay estimators over the three channels displayed in Figure 2. The simulation results are summarized in Figures 3 – 8. Figures 3 – 5 show the simulated mean of the five estimators over the three channels, respectively. All five perform reasonably well up to ± 60 kHz. Here, the Fitz and M&M estimators stop tracking. The ESP, L&R, and Kay estimators track up to ± 100 kHz (roughly 1% of the bit rate), except the Kay estimator shows some bias. This bias channel dependent and are traced back to inaccuracies in the approximation (28).

The simulated variances of the estimators are summarized in Figures 6 – 8 for the three channels, respectively. These results show that the Fitz, L&R, and M&M estimators achieve the same mean-squared error performance. The ESP estimator is a few dB worse than these three whereas the Kay estimator has the worst mean-squared error performance. This is not a surprising result for the Kay estimator given the fact that the approximation (28) is required.

VI. CONCLUSIONS

On the whole, the modified L&R estimator is the best in terms of tracking range and achievable mean-squared error. The ESP estimator is a close second and offers a computational complexity advantage in that it only requires the computation of one correlation value as opposed to the five correlation values required by the L&R estimator.

REFERENCES

- [1] Integrated Network Enhanced Telemetry (iNET) Radio Access Network Standards Working Group, "Radio access network (RAN) standard, version 0.7.9," Tech. Rep., available at <https://www.tenadsa.org/display/INET/iNET+Platform+Interface+Standards>.
- [2] D. Rife and R. Boorstyn, "Single tone parameter estimation from discrete-time observations," *IEEE Transactions on Information Theory*, vol. 20, no. 5, p. 591, September 1974.
- [3] S. Kay, "A fast and accurate single frequency estimator," *IEEE Transactions on Acoustics, Speech, and Signal Processing*, vol. 37, no. 12, pp. 1987–1990, December 1989.
- [4] M. Fitz, "Further results in the fast estimation of a single frequency," *IEEE Transactions on Communications*, vol. 42, no. 2/3/4, p. 862, February/March/April 1994.
- [5] M. Luise and R. Reggiannini, "Carrier frequency recovery in all-digital modems for burst-mode transmissions," *IEEE Transactions on Communications*, vol. 43, no. 2/3/4, p. 1169, February/March/April 1995.
- [6] U. Mengali and M. Morelli, "Data-aided frequency estimation for burst digital transmission," *IEEE Transactions on Communications*, vol. 45, no. 1, p. 23, January 1997.
- [7] f. harris and C. Dick, "Preamble structure for fast acquisition and equalization of QAM signals," in *Proceedings of the SDR'09 Technical Conference and Product Exposition*, Washington, DC, 1–4 December 2009.
- [8] B. Erkmen, A. Tkachenko, and C. Okino, "Preamble design for symbol timing estimation from SOQPSK-TG waveforms," in *Proceedings of the International Telemetry Conference*, Las Vegas, NV, October 2009.
- [9] E. Perrins and M. Rice, "Reduced-complexity approach to iterative detection of coded SOQPSK," *IEEE Transactions on Communications*, vol. 55, pp. 1354–1362, July 2007.
- [10] T. Nelson, E. Perrins, and M. Rice, "Near optimal common detection techniques for shaped offset QPSK and Feher's QPSK," *IEEE Transactions on Communications*, vol. 56, pp. 724–735, May 2008.
- [11] P. Schreier and L. Scharf, *Statistical Signal Processing of Complex-Valued Data*. New York: Cambridge University Press, 2010.
- [12] U. Mengali and A. D'Andrea, *Synchronization Techniques for Digital Receivers*. New York: Springer, 1997.
- [13] M. Rice and M. Jensen, "A comparison of L-band and C-band multipath propagation at Edwards AFB," in *Proceedings of the International Telemetry Conference*, Las Vegas, NV, October 2011.

APPENDIX

Here, the derivation of (8) is outlined. Starting with the definition (7) and using $\delta = dL_q$ gives

$$R(dL_q) = \frac{1}{(6-d)L_q} \sum_{n=i+L_q+\delta}^{i+7L_q-1} r(n)r^*(n-\delta) \quad (30)$$

Using the indexes (5), $R(dL_q)$ may be re-written as

$$R(dL_q) = \frac{1}{(6-d)L_q} \sum_{\ell=d+1}^6 \sum_{m=0}^{L_q-1} r(i+\ell L_q+m)r^*(i+(\ell-d)L_q+m). \quad (31)$$

Substituting the relationship for $r(n)$ given in (6) and rearranging gives

$$R(dL_q) = \frac{1}{(6-d)L_q} \sum_{\ell=d+1}^6 \sum_{m=0}^{L_q-1} |\alpha(m)|^2 e^{jdL_q\omega_0} + \frac{1}{(6-d)L_q} \sum_{\ell=d+1}^6 \sum_{m=0}^{L_q-1} [v_1(\ell, m) + v_2(\ell, m) + v_3(\ell, m)]. \quad (32)$$

The first term in (32) may be simplified as

$$\frac{1}{(6-d)L_q} \sum_{\ell=d+1}^6 \sum_{m=0}^{L_q-1} |\alpha(m)|^2 e^{jdL_q\omega_0} = \frac{\alpha^2}{L_q} \quad (33)$$

where

$$\alpha^2 = \sum_{m=0}^{L_q-1} |\alpha(m)|^2. \quad (34)$$

The second term in (32) involves the double summation of three noise terms. The first of these noise terms is

$$v_1(\ell, m) = \alpha(m)e^{j(i+\ell L_q+m)\omega_0} w^*(i+(\ell-d)L_q+m) \quad (35)$$

which is a complex-valued Gaussian random variable with variance $|\alpha(m)|^2 \sigma_w^2$ [see (2)]. Similarly,

$$v_2(\ell, m) = \alpha^*(m)e^{-j(i+(\ell-d)L_q+m)\omega_0} w(i+\ell L_q+m) \quad (36)$$

is also a complex-valued Gaussian random variable with variance $|\alpha(m)|^2 \sigma_w^2$. Furthermore, given the assumption that the $w(n)$ are a sequence of uncorrelated *proper* complex-valued Gaussian random variables, $v_1(\ell, m)$ and $v_2(\ell, m)$ are uncorrelated [11]. The last of the noise terms in (32) is

$$v_3(\ell, m) = w(i+\ell L_q+m)w^*(i+(\ell-d)L_q+m). \quad (37)$$

Here we make the assumption² that for sufficiently high signal-to-noise ratios (i.e., sufficiently small σ_w^2), this product term is much smaller than the first two terms with high probability. Consequently, the product term may be neglected and we are left with

$$v \approx \frac{1}{(6-d)L_q} \sum_{\ell=d+1}^6 \sum_{m=0}^{L_q-1} [v_1(\ell, m) + v_2(\ell, m)] \quad (38)$$

which is the sum of uncorrelated complex-valued Gaussian random variables each with zero mean and variance $|\alpha(m)|^2 \sigma_w^2$. Consequently, v is complex-valued Gaussian random variable with zero mean and variance

$$\sigma_v^2 = \frac{2\alpha^2}{L_q^2} \sigma_w^2. \quad (39)$$

²This is a standard assumption in the frequency estimation literature. See [3], [4], [5], [6].

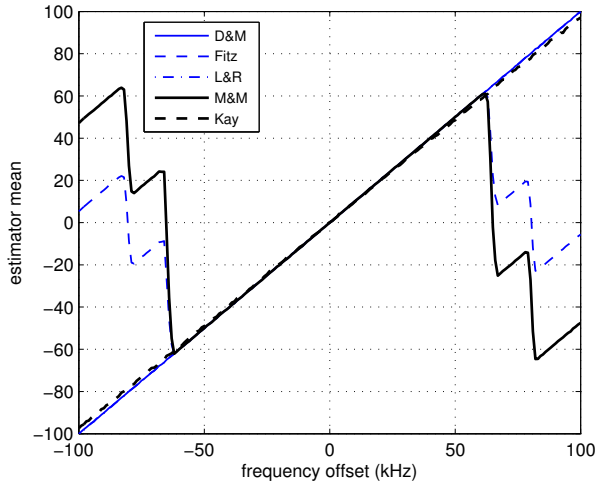


Fig. 3. Estimator means for the first channel of Figure 2. For these simulations $E_b/N_0 = 15$ dB.

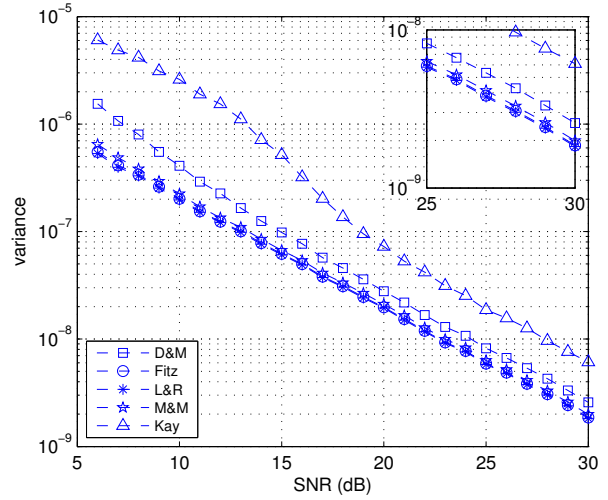


Fig. 6. Estimator variances for the first channel of Figure 2.

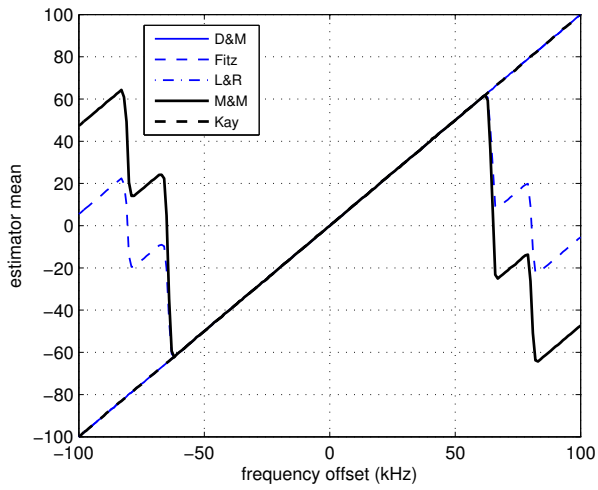


Fig. 4. Estimator means for the second channel of Figure 2. For these simulations $E_b/N_0 = 15$ dB.

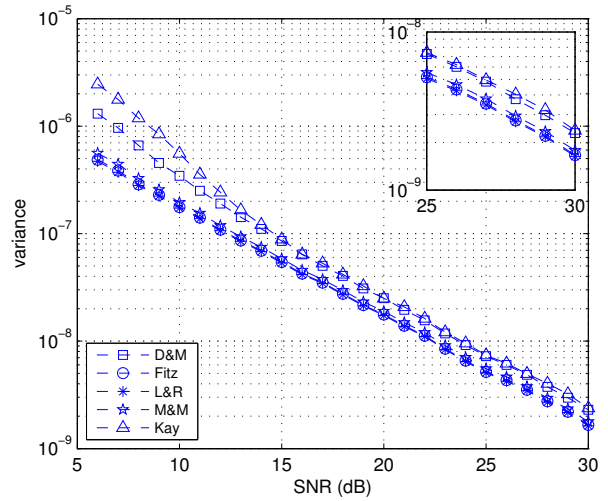


Fig. 7. Estimator means for the second channel of Figure 2.

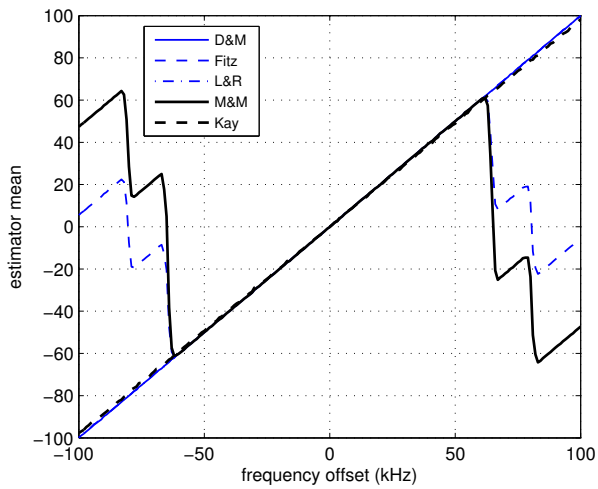


Fig. 5. Estimator means for the third channel of Figure 2. For these simulations $E_b/N_0 = 15$ dB.

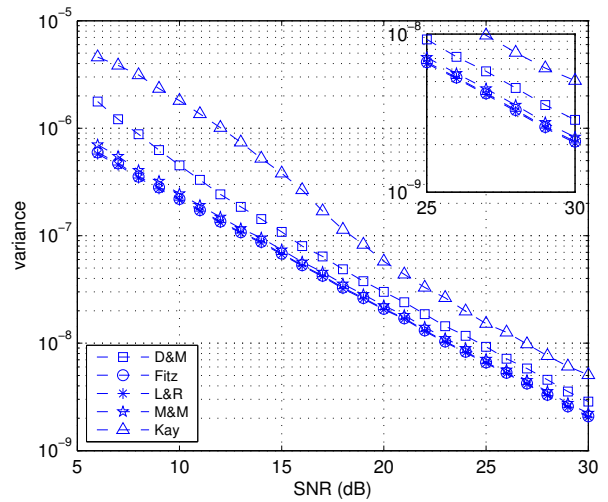


Fig. 8. Estimator means for the third channel of Figure 2.